



Cite this: *RSC Adv.*, 2023, 13, 11929

Uranyl nitrate as a recyclable homogeneous photocatalyst for selective cross-coupling of *N*-substituted amines and indoles†

Shuaipeng Lv,^{‡,ab} Qiannan Li,^{‡,ab} Ji-Wei Sang,^b Yu Zhang,^{*a} Jinxin Wang^{ID} ^{*ab} and Wei-Dong Zhang^{ID} ^{*ab}

A homogeneous photocatalytic recyclable system for the selective radical–radical cross-coupling of *N*-substituted amines and indoles has been established. This system could conduct in water or acetonitrile, featuring the reuse of uranyl nitrate as the recyclable photocatalyst *via* a simple extraction. With this mild strategy in hand, good to excellent yields of cross-coupling products could be achieved even under the irradiation of sunlight, including 26 natural product derivatives and 16 natural product inspired re-engineered compounds. A radical–radical cross-coupling mechanism was newly proposed based on experimental evidence and reported literature. This strategy has been also applied to a gram scale synthesis to demonstrate its practical utility.

Received 15th February 2023
Accepted 5th April 2023

DOI: 10.1039/d3ra01037f

rsc.li/rsc-advances

Introduction

In the past decades, great effort has been devoted to accessing sustainability in organic syntheses, such as by using metal-free strategies, green solvents, recyclable catalysts, photocatalysis, *etc* (Fig. 1A).¹ Among them, recycling and reusing the catalyst is a highly interesting alternative to achieve the goal of green synthesis. Generally, homogeneous catalysts have better activities, while they are rarely recycled because of the difficulty of separation from the solvent,² thereby resulting in the waste of catalysts and solvents in most homogeneous catalysis (Fig. 1B). To overcome these, several elegant strategies have been reported to achieve this goal, all these methods can be summed up in two main solutions, homogeneous catalysis and heterogeneous separation, and heterogenized (immobilized) homogeneous catalysts.³ The most popular strategy is the water-based recycling catalysis system,⁴ such as water-soluble catalysts in an aqueous/organic biphasic system,^{5,6} even in switchable water.⁷ However, application to diverse organic transformations are still underexplored.

Photoredox reactions in water have elicited increasing interest.^{8–11} However, only a few examples regarding recycling

catalysts in water have been reported and mainly concentrated on micellar catalysis or heterogeneous catalysts in water.^{12–15} Uranyl cations ($^{238}\text{UO}_2^{2+}$) were recently emerging as an ideal

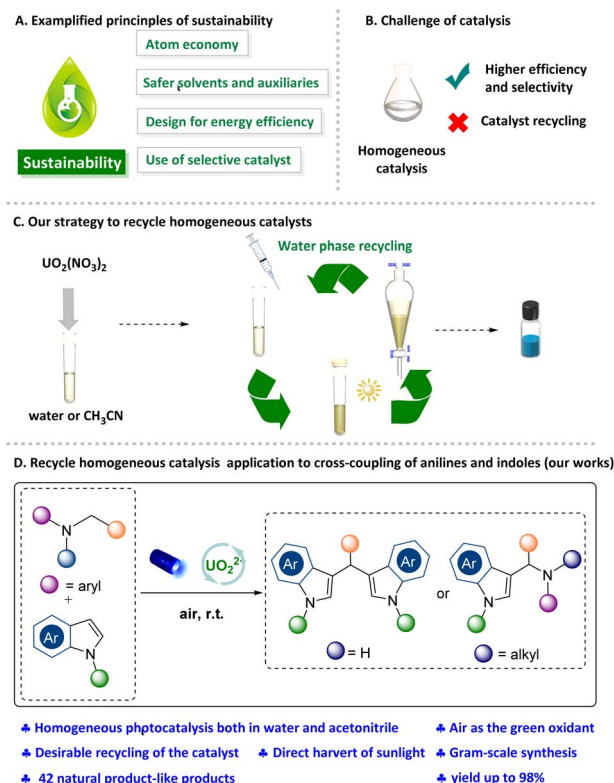


Fig. 1 Homogeneous photocatalyzed chemical transformation via a recyclable uranyl nitrate in water or CH_3CN .

^aShanghai Frontiers Science Center for Chinese Medicine Chemical Biology, Institute of Interdisciplinary Integrative Medicine Research, Shanghai University of Traditional Chinese Medicine, No. 1200, Cailun Road, Shanghai 201203, China. E-mail: yzhang@shutcm.edu.cn; dzhangy@hotmail.com

^bSchool of Pharmacy, Second Military Medical University, Shanghai 200433, China. E-mail: jxwang2013@126.com

† Electronic supplementary information (ESI) available. CCDC 2124830 2220117. For ESI and crystallographic data in CIF or other electronic format see DOI: <https://doi.org/10.1039/d3ra01037f>

‡ These authors contributed equally to this work.



water-soluble photoredox catalysts.^{16,17} It should be noted that uranyl cations have obvious solubility difference in solvents especially the excellent solubility in water and acetonitrile. However, it showed strongly limited solubility in many solvents such as dichloromethane and ethyl acetate. Although a few excellent organic transformations using uranyl cations were reported recently,^{18–22} it is still untapped to recycle and reuse it in organic synthesis. Moreover, uranyl cations, activated by visible-light irradiation through ligand-to-metal charge transfer (LMCT), achieves the unique characteristic of excellent oxidizing ability ($E^\circ = +2.36$ V vs. SCE), were successfully used to selectively oxidation of sulfides,¹⁸ the photocatalyzed hydrolysis of diaryl ethers,¹⁹ activate the C–N bond of protogenetic anilines, tertiary anilines to form phenols *via* a single electron transfer (SET) process.²⁰

Single electron oxidation of amines provides an efficient way to access synthetically useful α -aminoalkyl radicals as reactive intermediates. The generated α -aminoalkyl radicals has been utilized in a variety of reaction systems to form several important bonds such as C–C, C–N, C–O, and C–P.^{23,24} The presence of amines in numerous alkaloids, pharmaceuticals, and agrochemicals lends credence to the potential utility of this chemistry in construction of functional molecular libraries.²⁵ Inspired by these, we aim to develop an elegant and mild strategy enabling reuse the uranyl nitrate based on its specific solubleness and photochemical characteristics (Fig. 1C). Herein, two efficient radical cross-coupling reactions between anilines and indoles were developed using the uranyl nitrate as photocatalyst for multiple times with maintaining performance, which different from the previous works in term of mechanism (Fig. 1D).


Our investigation into this new recyclable homogeneous photoredox catalysis began with SET oxidative cross-coupling of secondary anilines with indoles. We commenced our studies with secondary anilines *N*-aryl glycine ethyl ester (**1a**) and indole

(**2a**) as model substrates (Table 1). Uranyl cation was used as the photocatalyst under the irradiation of blue LEDs ($\lambda_{\max} = 456$ nm), in which CH_3CN was added as the homogeneous phase. To our delight, we found that uranyl nitrate hexahydrate in CH_3CN under air atmosphere with TFA exhibited the best reactivity, and afforded desired product **3a** in 96% isolated yield (entry 1). Replacing the photocatalyst resulted in diminished efficiency (57% yield, entry 2). We also attended to changing the solvent into the water, however, only 20% desired product was detected (entry 3). Of note, the catalyst was recycled from water phase during the work-up, which exhibited comparable reactivity (entry 4). Moreover, the absence of the oxygen and the photocatalyst, visible light or acid, exhibited lower reactivity, respectively (entries 5–8). These control experiments indicated that photocatalyst, air, visible light and acid are essential for this reaction.

With the best-optimized conditions in hand, the scope was further explored to determine the generality (Scheme 1). Initially, we explored the scope of indoles in this tandem reaction. Various substrates bearing functional groups at the indoles motif (**1b–1k**) underwent smoothly and delivered expected disindoles products (**3b–3k**) in good to excellent yields. Specifically, electrically neutral or electron-rich indoles (**2b–2d**) performed well (**3b–3d**, 97–99% yields). It is worth noting that, halogen substituents on indoles, even a photosensitive iodine moiety (**3e–3h**, 74–95% yields) were well tolerated under the standard conditions. Notably the efficiency of the reaction was not impeded by strong electron-deficient substituents such as nitro (**3i**), cyano (**3j**) and ester (**3k**) (53–94% yields). Subsequently, the substrate scope of anilines for this photocatalytic coupling reaction was also evaluated. Firstly, a range of esters, including *t*-butyl ester, benzyl ester, icariidin ester, cholesteryl ester and 1,4-butyrolactone can be readily employed in this reaction to afford the products with good to excellent yield (**3l–3p**, 71–93% yields), and the structure of **3m** was further confirmed by a single crystal X-ray analysis. Perhaps most importantly, this transformation is not limited to glycine derivatives.²⁶ For example, *N*-benzyl or *N*-alkyl substituted anilines were found to be suitable substrates. The reaction of unsubstituted indole **2a** with *N*-benzyl-4-methoxyaniline (**1q**) selectively afforded 3,3'-(phenylmethylene)bis(1*H*-indole) (**3q**), which acts as an antibiotic natural product named turbomycin B in 54% isolated yield.²⁷ In addition, *N*-benzylic anilines bearing an electron-donating substituent such as methoxy and *t*-butyl groups or electron-deficient trifluoromethyl group could also be incorporated (**3r–3u** 41–66% yields). It is noteworthy that product **3r** is an orphan nuclear receptor inhibitor²⁸ and product **3t** acts as antileukemic agent.²⁹ **3u** shows an inhibition of renal cell carcinoma.³⁰ Moreover, heteroaromatic *N*-benzylic anilines also reacted efficiently with **2a** to afford the arindoline A (**3v**) and turbomycin A (**3w**) (74% and 65% yields respectively). Pleasingly, *N*-alkyl-anilines such as ethyl, *n*-butyl, 1-pentanol were also reactive and afforded vibrindole A (**3x**), ST-1385 (**3y**) and streptindole (**3z**) in 17%, 32% and 15% yields.

After the oxidative deaminative dimerization of second anilines and indoles, we further examined the SET oxidation of tertiary anilines with indoles.^{31–33} We initialed our studies with

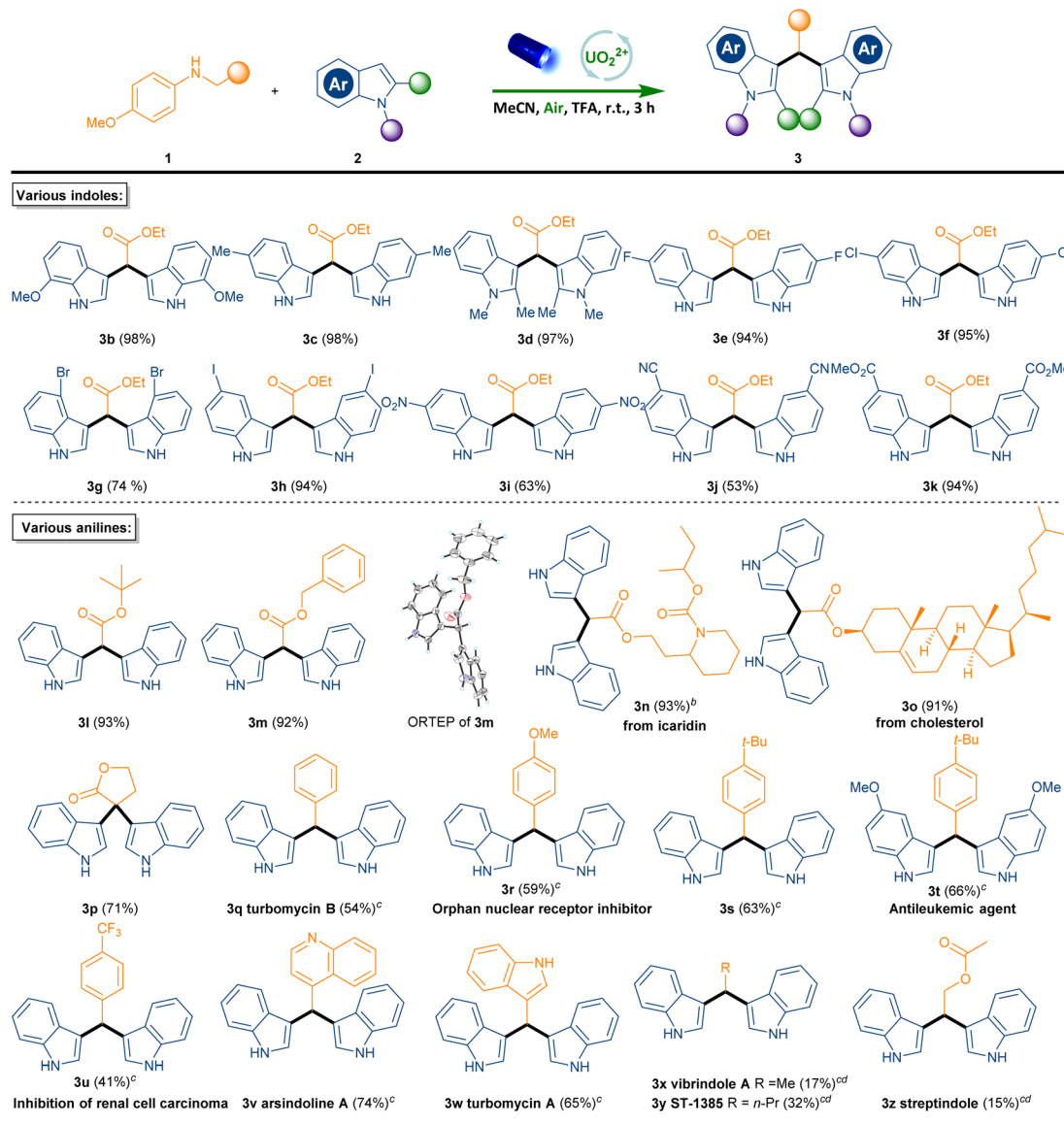
Table 1 Optimization of SET oxidative cross-coupling of secondary anilines with indoles^a



Entry	Conditions	Yield (%)
1	$\text{UO}_2(\text{NO}_3)_2 \cdot 6\text{H}_2\text{O}$	96
2	$\text{UO}_2(\text{OAc})_2 \cdot 2\text{H}_2\text{O}$	57
3	H_2O instead of MeCN	20
4	Recycled catalyst ^b	91
5	Under Ar	22
6	Without $\text{UO}_2(\text{NO}_3)_2 \cdot 6\text{H}_2\text{O}$	0
7	Without light	26
8	Without TFA	18

^a Reaction conditions: **1a** (1.0 equiv.), **2a** (2.1 equiv.), photocatalyst (4 mol%), TFA (2.0 equiv.), MeCN (0.05 M), room temperature, Blue LEDs (456 nm 40 W), 3 h. ^b Obtained by lyophilization of the water phase from extraction.





Scheme 1 Scope of indoles and anilines.^a Reaction conditions: 1 (1.0 equiv.), 2 (2.1 equiv.), photocatalyst (4 mol%), TFA (2.0 equiv.), MeCN (0.05 M), room temperature, blue LEDs (456 nm, 40 W) for 3 h.^b For 10 h.^c For 16 h.^d Photocatalyst (8 mol%).

N-phenyl-tetrahydroisoquinoline (**4a**) and 1,2-dimethyl-1*H*-indole (**2d**) as model substrates (Table 2). Under the same condition, the cross-coupling product **5a** was obtained in 96% yield within 6 h and the TFA was found to be useless (entry 1). The structure of **5a** was further confirmed by a single crystal X-ray analysis. To our delight, this transformation could be conducted in the water with same yield (entry 2). Therefore, the recycled water phase from extraction could be directly reused for the next reaction with same reactivity (entry 3). Later, the absence of oxygen and the photocatalyst exhibited lower reactivity, respectively (entries 4, 5). No formation of the product in the dark strongly proved the necessity of the light (entry 6). Furthermore, reducing the amount of **4a** or photocatalyst slightly decreased the yield (entries 7, 8). With the best-

optimized conditions in hand, the scope was further explored to determine the generality (Scheme 2).

Firstly, various substrates bearing functional groups at the tetrahydroisoquinoline motif **4b–4d** underwent smoothly standard conditions and delivered expected cross-coupling products **5b–5d** in good to excellent yields. It was noteworthy that *N*-substituted 4,5,6,7-tetrahydrothieno [3,2-*c*] pyridine, a core structure of popular medicines such as (*S*)-clopidogrel³⁴ and prasugrel,³⁵ could afford the corresponding product in 76% yield (**5e**). Afterwards, a variety of *N*-aryl-tetrahydroisoquinolines containing diverse substituted aromatic rings was tolerated satisfactorily (**5f–5j**). Notably, the electronic properties of 4-substituted groups on the phenyl ring have an unobvious effect on the reaction performance. Interestingly, those products were highly potential intermediates for

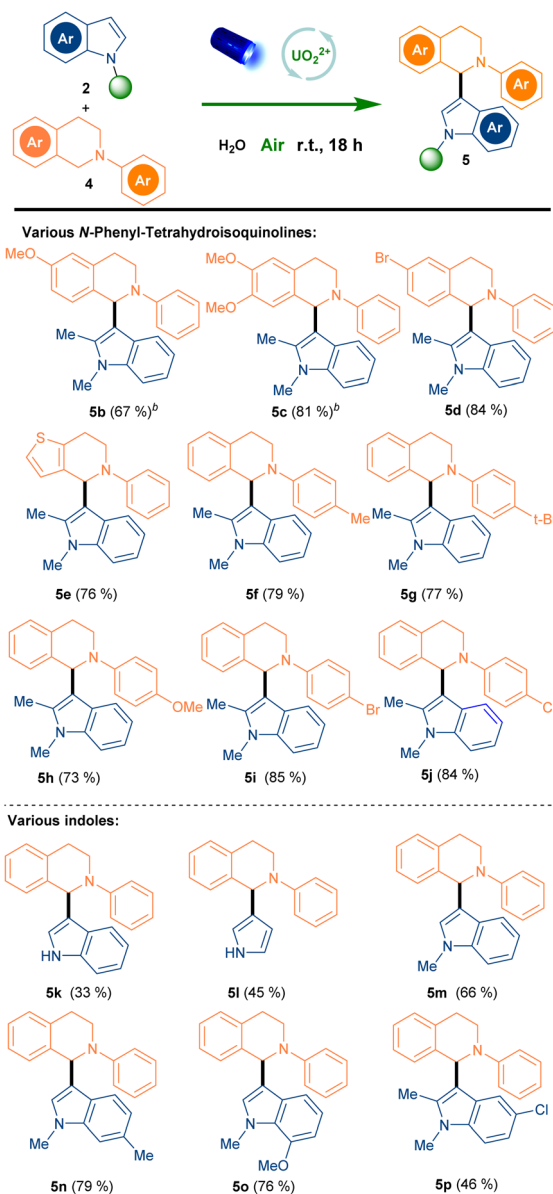
Table 2 Optimization of the reaction conditions^a

Entry	Variations	Yield (%)
1	Acetonitrile as solvent, 6 h	95
2	—	96
3	Recycled water phase ^b	93
4	Under Ar	11
5	Without $\text{UO}_2(\text{NO}_3)_2 \cdot 6\text{H}_2\text{O}$	23
6	Dark at 40 °C	0
7	4a (1.5 equiv.)	81
8	$\text{UO}_2(\text{NO}_3)_2 \cdot 6\text{H}_2\text{O}$ (4 mol%)	69

^a Reaction conditions: **1a** (2.0 equiv.), **2a** (1.0 equiv.), $\text{UO}_2(\text{NO}_3)_2 \cdot 6\text{H}_2\text{O}$ (8 mol%) and H_2O (1.0 mL), blue LEDs (456 nm, 40 W), 18 h. ^b Water phase from extraction was directly used.

further functionalization. Meanwhile, various substituted indoles were examined under standard conditions. Among them, the indole and pyrrole without protection suppressed the reactivity greatly (**5k**, **5l**), probably due to the stability of indole radical.³⁶ However, indoles containing electron-donating groups proceeded efficiently (**5m–5o**). Indoles containing weak electron-withdrawing groups exhibited reactivity (**5p**). Moreover, stronger electron-withdrawing groups such as acyl group, nitro group at the 5 or 6 positions of indoles lead to no reaction at all (**5q–5s**).

To shed light on the mechanism and uncover the unique photooxidation properties of excited uranyl cation, radical quenching experiments with 2,2,6,6-tetramethyl-1-piperidinyloxy (TEMPO) as the radical quencher were carried out. Indeed, both reactions were suppressed and the TEMPO-trapped anilines and indole radical were detected by HRMS analysis, which indicated that the radical process was possible involved in our reaction (Scheme 3A and S2†). Furthermore, the uranyl cation was approved to serve as a photosensor *via* UV-vis absorption at 420 nm (Fig. 2A and C). Stern–Volmer analysis was further performed to uncover the species of active uranyl cation was quenched by **1a**, **2a**, **2d** and **4a** (Fig. 2B and D). Indole **2a** and **2d** have been widely shown to act as quenchers in visible-light mediated reactions, involved in the reaction in the form of allyl radicals.^{36,37} Combining all of results, it was suggested that the reaction was initiated with excited uranyl cation. Most of reported literature³² involved cross-coupling between the indoles and anilines gave a formal Mannich process, and in their system, the indole radical cannot form for the low excited state oxidation potential of photocatalysts ($E^\circ = +1.16$ V vs. SCE, for indole).³⁸ So alternative mechanistic pathways need to be considered. To further confirm the possible pathway, control experiments were carried out. The trimer of indole **2a'**, the dimer of tetrahydroisoquinoline (**4a'**)



Scheme 2 Scope of tetrahydroisoquinolines and indoles.^a Reaction conditions: **4** (2.0 equiv.), **2** (1.0 equiv.), photocatalyst (8 mol%), H_2O (1.0 mL), room temperature, blue LEDs (456 nm, 40 W) for 18 h. ^b **4** was added *via* a solution in MeCN (50 μL) (these tetrahydroisoquinolines need to be dispersed into water by MeCN).

and 2-indole-substituted 3-oxindole (**2d'**) were obtained under standard reaction conditions (CH_3CN or water as solvent, respectively) in the absence of a coupling partner, respectively.^{32a,37c–e,39} (Scheme 3B–D) The mixture of **4ab** and **4ab'** could be isolated under O_2 atmosphere,^{32a,39} even in the presence of a solvent amount of nucleophile (acetone), and formal Mannich product was not detected.^{32f,40} (Scheme 3E). Although cross coupling reaction involved indole radical is rarely reported,^{26a,41} In our uranyl nitrate system, the radical–radical coupling process was preferred. Moreover, the Manich type reaction between unactivated indoles and imines need very harsh condition.^{37c,42} On the basis of the above results and



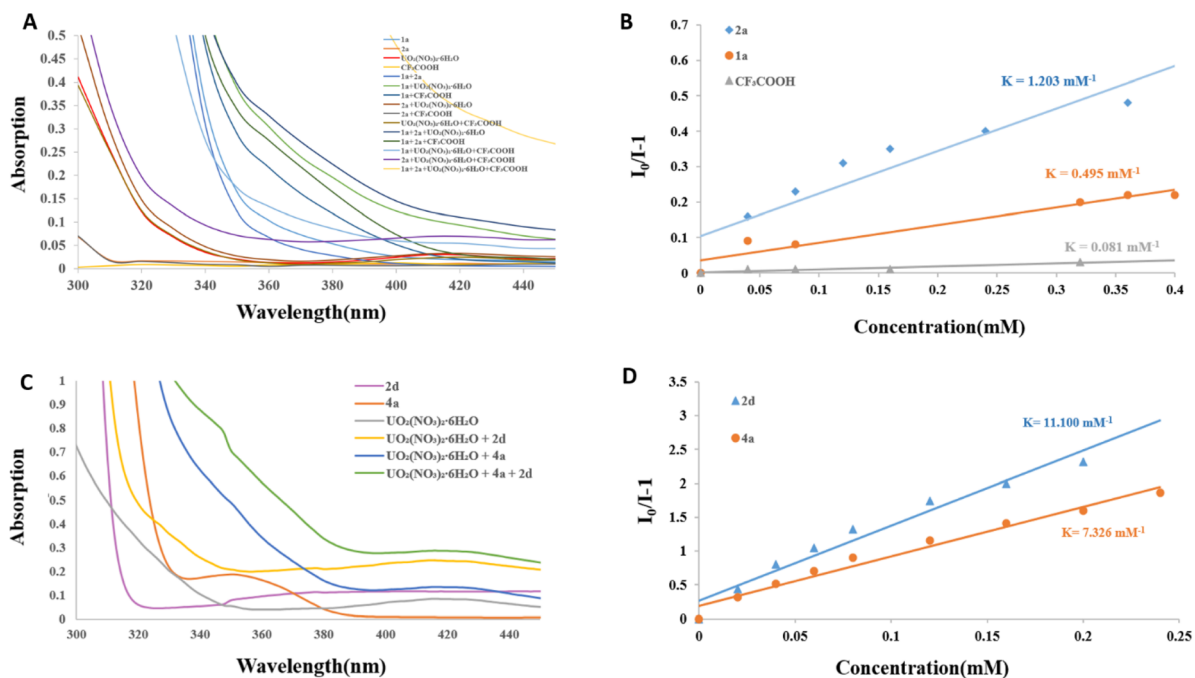
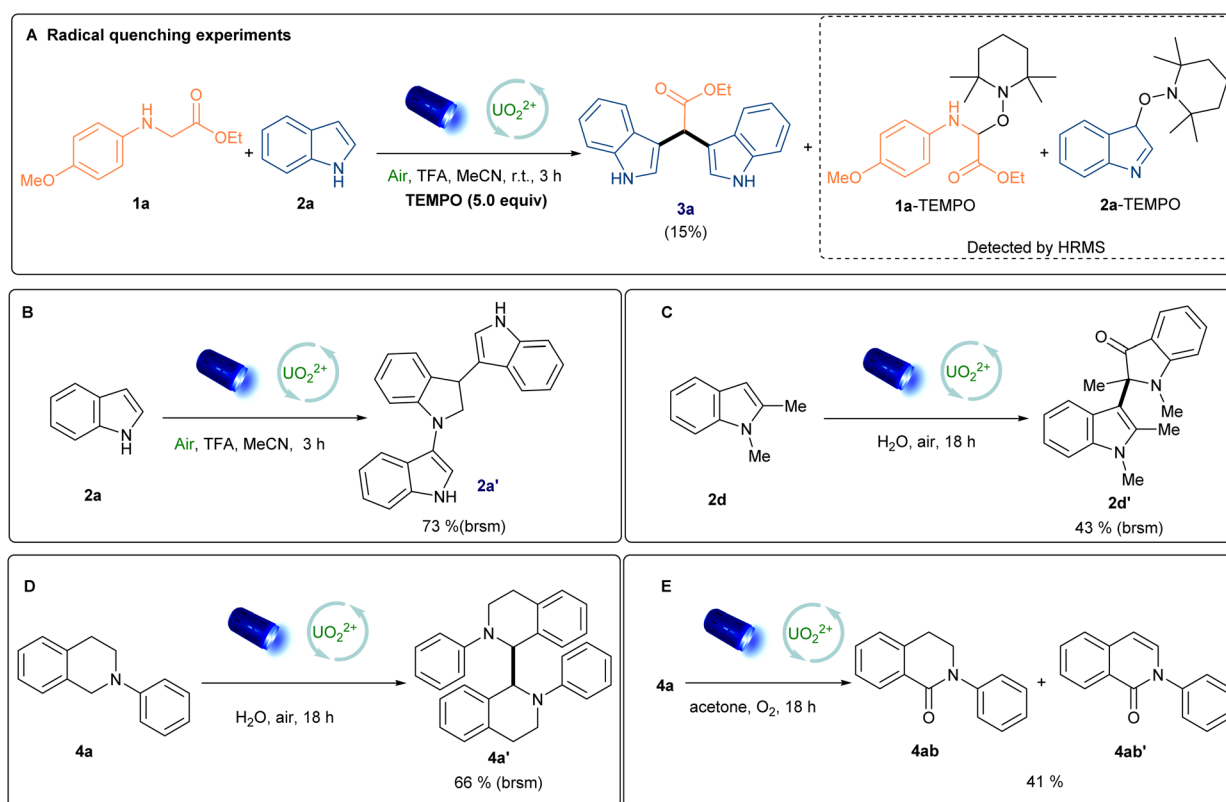


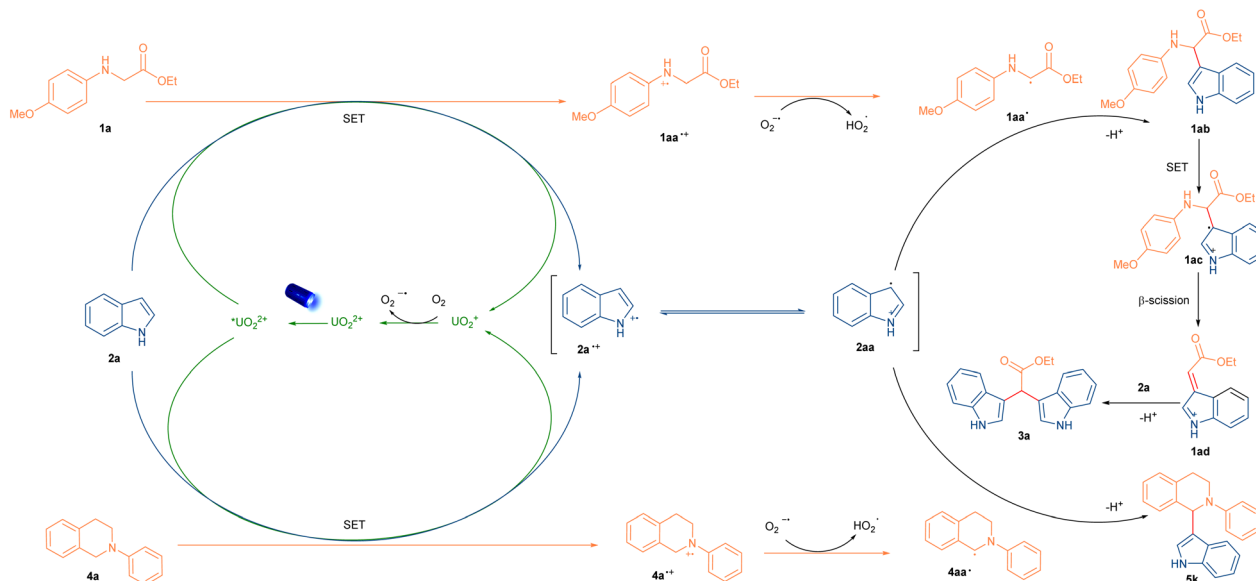
Fig. 2 UV-vis experiments and Stern–Volmer plot of fluorescence quenching experiment.

reported literature,^{26a,41} we proposed a plausible radical–radical coupling mechanism as shown in Scheme 4. Firstly, the excited $^*\text{UO}_2^{2+}$ ion is generated upon the irradiation of blue light. In

this process, excited $^*\text{UO}_2^{2+}$ promotes the SET oxidation of indole 2a and 2°, 3° anilines (1a and 4a) to generate corresponding radical cations. Meanwhile, UO_2^{2+} intermediate



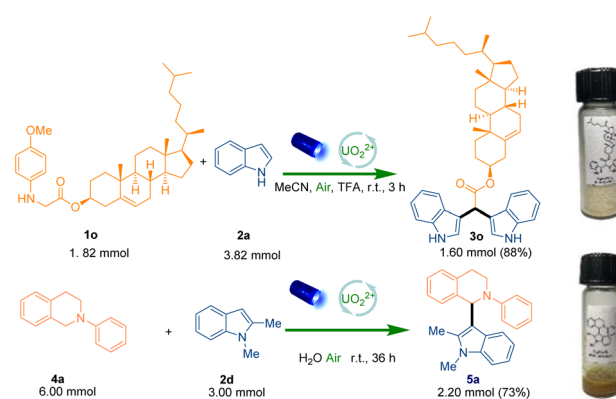
Scheme 3 Radical quenching experiments and control experiments.



Scheme 4 Proposed mechanism of cross coupling reactions of *N*-substituted amines and indoles.

reacted with O_2 to produce the superoxide radical anion ($O_2^{\cdot-}$) and further regenerate UO_2^{2+} . The α -aminoalkyl radicals **1aa'** and **4aa'** were subsequently formed after the deprotonation from HOO^{\cdot} radical. Radical **4aa'** could further coupled with intermediate **2aa** to generate desirable product **5a**. For reaction with **2o** anilines, **1aa'** will further react with **2aa** to form the intermediate the **1ab**, which undergoes an SET oxidative and β -scission to generate the **1ad**. Then it will be trapped by the purposely added nucleophile indole **2a** to afford desired product **3a** after deprotonation. However, alternative mechanistic pathways should not be fully excluded.

After the understanding of the reaction mechanism, the recyclability of UO_2^{2+} in the system was further investigated and a convenient recycle process was showcased. The simple work-



Scheme 5 Gram-scale synthesis **3o** and **5a**.

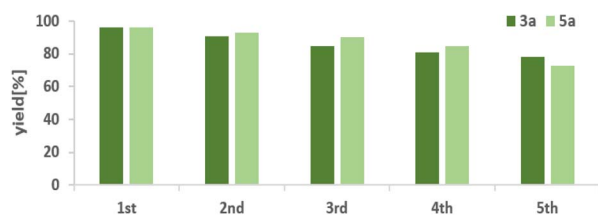
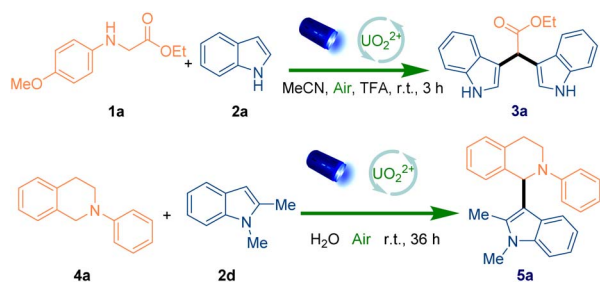


Fig. 3 Recyclability of UO_2^{2+} in the reactions for the generation of **3a** and **5a**.

up (extraction with water and dichloromethane three times) was carried out to remove the organic reagents after the completion of reaction, and then the water phase containing the water-soluble photocatalyst could be reused for the next reaction cycle. Delightedly, five recycling cycles were performed which showed the stable performance of recycled homogeneous photocatalytic system (Fig. 3). To further exploit other characteristics of sustainability, the reactions were also conducted in excellent yield *via* harvesting the sunlight (95% and 94% yield respectively) (Scheme S6 and S7[†]). Finally, gram-scale (3.0 mmol) reactions (Scheme 5) were carried out, which afforded the target product in 88% and 73% yield respectively.

Conclusions

In summary, we have developed a highly mild and environmentally benign strategy for the construction of two types of natural product-like libraries by the selective cross-coupling of anilines and indoles. The homogeneous catalysis system is



keeping comparable performance after 5 recycling cycles *via* using water (acetonitrile)-soluble depleted uranium as the recycled photocatalyst. Although cross coupling reaction involved indole radical is rarely reported, in our uranyl nitrate system, the radical–radical coupling process was preferred based on experimental evidences and reported literature. Moreover, the reaction *via* harvesting the sunlight and gram-scale reaction strongly proved the practicability of this system. We believe this method enables the development of uranium enrichment catalysis and represents a lower-cost, milder organic transformation process.

Conflicts of interest

There are no conflicts to declare.

Acknowledgements

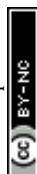
This work was supported by National Natural Science Foundation of China (No. 82003624, 82141203, 82004003, 82004215), Science and Technology Commission of Shanghai Municipality (No. 20YF1458700, 20YF1459000), Innovation Team and Talents Cultivation Program of National Administration of Traditional Chinese Medicine (ZYYCXTDD-202004) and Shanghai Frontiers Science Center of TCM Chemical Biology. We are also grateful to Dr Lu Lu for carrying out the NMR experiments.

Notes and references

- 1 S. Kar, H. Sanderson, K. Roy, E. Benfenati and J. Leszczynski, Green chemistry in the synthesis of pharmaceuticals, *Chem. Rev.*, 2022, **122**, 3637–3710.
- 2 G. Szöllösi, Asymmetric one-pot reactions using heterogeneous chemical catalysis: recent steps towards sustainable processes, *Catal. Sci. Technol.*, 2018, **8**, 389–422.
- 3 (a) J. G. de Vries and S. D. Jackson, Homogeneous and heterogeneous catalysis in industry, *Catal. Sci. Technol.*, 2012, **2**, 2009; (b) J.-D. Xia, G.-B. Deng, M.-B. Zhou, W. Liu, P. Xie and J.-H. Li, Reusable Visible Light Photoredox Catalysts; Catalyzed Benzylic C(sp³)-H Functionalization/Carbocyclization Reactions, *Synlett*, 2012, **23**, 2707–2713.
- 4 W. Wang, L. Cui, P. Sun, L. Shi, C. Yue and F. Li, Reusable *N*-heterocyclic carbene complex catalysts and beyond: a perspective on recycling strategies, *Chem. Rev.*, 2018, **118**, 9843–9929.
- 5 T. Rösler, T. A. Faßbach, M. Schrimpf, A. J. Vorholt and W. Leitner, Toward Water-based recycling techniques: methodologies for homogeneous catalyst recycling in liquid/liquid multiphase media and their implementation in continuous processes, *Ind. Eng. Chem. Res.*, 2019, **58**, 2421–2436.
- 6 C. W. Kohlpaintner, R. W. Fischer and B. Cornils, Aqueous biphasic catalysis: Ruhrchemie/Rhône-Poulenc oxo process, *Appl. Catal., A*, 2001, **221**, 219–225.
- 7 S. M. Mercer, T. Robert, D. V. Dixon and P. G. Jessop, Recycling of a homogeneous catalyst using switchable water, *Catal. Sci. Technol.*, 2012, **2**, 1315–1318.
- 8 J. Steinbauer, L. Longwitz, M. Frank, J. Epping, U. Kragl and T. Werner, Immobilized bifunctional phosphonium salts as recyclable organocatalysts in the cycloaddition of CO₂ and epoxides, *Green Chem.*, 2017, **19**, 4435–4445.
- 9 S. Barata-Vallejo, D. E. Yerien and A. Postigo, Advances in photocatalytic organic synthetic transformations in water and aqueous media, *ACS Sustainable Chem. Eng.*, 2021, **9**, 10016–10047.
- 10 M.-J. Bu, C. Cai, F. Gallou and B. H. Lipshutz, PQS-enabled visible-light iridium photoredox catalysis in water at room temperature, *Green Chem.*, 2018, **20**, 1233–1237.
- 11 K. Sun, Q.-Y. Lv, X.-L. Chen, L.-B. Qu and B. Yu, Recent advances in visible-light-mediated organic transformations in water, *Green Chem.*, 2021, **23**, 232–248.
- 12 D. Chen, J. Liu, X. Zhang, H. Jiang and J. Li, Recent advances in aqueous phase visible light catalytic reactions, *Chin. J. Org. Chem.*, 2019, **39**, 3353–3362.
- 13 B. Long, Z. Ding and X. Wang, Carbon nitride for the selective oxidation of aromatic alcohols in water under visible light, *ChemSusChem*, 2013, **6**, 2074–2078.
- 14 Z.-Y. Xu, Y. Luo, D.-W. Zhang, H. Wang, X.-W. Sun and Z.-T. Li, Iridium complex-linked porous organic polymers for recyclable, broad-scope photocatalysis of organic transformations, *Green Chem.*, 2020, **22**, 136–143.
- 15 J.-W. Cui, S. Ma, C.-H. Rao, M.-Z. Jia, X.-R. Yao and J. Zhang, Reusable homogeneous metal- and additive-free photocatalyst for high-performance aerobic oxidation of alcohols to carboxylic acids, *Appl. Catal., B*, 2022, **305**, 121028.
- 16 D. Q. Hua and X. F. Jiang, Perspectives for uranyl photoredox catalysis, *Synlett*, 2021, **32**, 1330–1342.
- 17 B. E. Cowie, J. M. Purkis, J. Austin, B. Jason, J. B. Love and P. L. Arnold, Thermal and photochemical reduction and functionalization chemistry of the uranyl dication, [U^{VI}O₂]²⁺, *Chem. Rev.*, 2019, **119**, 10595–10637.
- 18 Y. Li, S. A.-e.-A. Rizvi, D. Hu, D. Sun, A. Gao, Y. Zhou, J. Li and X. Jiang, Selective Late-Stage Oxygenation of Sulfides with Ground-State Oxygen by Uranyl Photocatalysis, *Angew. Chem., Int. Ed.*, 2019, **58**, 13499–13506.
- 19 D. Hu, Y. Zhou and X. Jiang, From aniline to phenol: carbon-nitrogen bond activation via uranyl photoredox catalysis, *Nat. Sci. Rev.*, 2021, nwab156.
- 20 Y. Mao, Y. Liu, L. Yu, S. Ni and Y. Pan, Uranyl-catalysed C–H alkynylation and olefination, *Org. Chem. Front.*, 2021, **8**, 5968–5974.
- 21 Y. Zhou, D. Hu, D. Li and X. Jiang, Uranyl-photocatalyzed hydrolysis of diaryl ethers at ambient environment for the directional degradation of 4-O-5 lignin, *J. Am. Chem. Soc.*, 2021, **1**, 1141–1146.
- 22 D. Hu and X. Jiang, Stepwise Benzylic Oxygenation via Uranyl-Photocatalysis, *Green Chem.*, 2022, **24**, 124–129.
- 23 J. W. Beatty and C. R. J. Stephenson, Amine Functionalization via Oxidative Photoredox Catalysis: Methodology Development and Complex Molecule Synthesis, *Acc. Chem. Res.*, 2015, **48**, 1474–1484.
- 24 K. Nakajima, Y. Miyake and Y. Nishibayashi, Synthetic Utilization of α -Aminoalkyl Radicals and Related Species in



- Visible Light Photoredox Catalysis, *Acc. Chem. Res.*, 2016, **49**, 1946–1956.
- 25 (a) G. Karageorgis, D. J. Foley, L. Laraia, S. Brakmann and H. Waldmann, Pseudo Natural Products—Chemical Evolution of Natural Product Structure, *Angew. Chem., Int. Ed.*, 2021, **60**, 15705–15723; (b) M. Grigalunas, S. Brakmann and H. Waldmann, Chemical Evolution of Natural Product Structure, *J. Am. Chem. Soc.*, 2022, **144**, 3314–3329.
- 26 (a) M. D'Auria, Photochemical synthesis of diindolylmethanes, *Tetrahedron*, 1991, **41**, 9225–9230; (b) S. D. Jadhav, D. Bakshi and A. Singh, Visible Light Mediated Organocatalytic Activation of Ethyl Bromofluoroacetate: Coupling with Indoles and Anilines, *J. Org. Chem.*, 2015, **80**, 10187–10196; (c) Y. Zhang, X. Yang, H. Zhou, S. Li, Y. Zhu and Y. Li, Visible light-induced aerobic oxidative cross-coupling of glycine derivatives with indoles: a facile access to 3,3' bisindolylmethanes, *Org. Chem. Front.*, 2018, **5**, 2120–2125; (d) T. Yang, H. Lu, Y. Shu, Y. Ou, L. Hong, C. T. Au and R. Qiu, CF₃SO₂Na-Mediated, UV-Light-Induced Friedel–Crafts Alkylation of Indoles with Ketones/Aldehydes and Bioactivities of Products, *Org. Lett.*, 2020, **22**, 827–831; (e) F. Stanek, R. Pawlowski, P. Morawska, R. Bujok and M. Stodulski, Dehydrogenation and α -functionalization of secondary amines by visible-light-mediated catalysis, *Org. Biomol. Chem.*, 2020, **18**, 2103–2112; (f) Y. Zhu, S. Li, X. Yang, S. Wang and Y. Zhang, Direct Synthesis of Triphenylamine-based Ordered Mesoporous Polymers for Metal-Free Photocatalytic Aerobic Oxidation, *J. Mater. Chem. A*, 2022, **10**, 13978–13986.
- 27 D. E. Gillespie, S. F. Brady, A. D. Bettermann, N. P. Cianciotto, M. R. Liles, M. R. Rondon, J. Clardy, R. M. Goodman and J. Handelsman, Isolation of antibiotics turbomycin A and B from a metagenomic library of soil microbial DNA, *Appl. Environ. Microbiol.*, 2002, **68**, 4301–4306.
- 28 S. Chintharlapalli, R. Burghardt, S. Papineni, S. Ramaiah, K. Yoon and S. Safe, Activation of Nur77 by selected 1,1-Bis(3'-indolyl)-1-(*p*-substituted phenyl)methanes induces apoptosis through nuclear pathways, *J. Biol. Chem.*, 2005, **280**, 24903–24914.
- 29 R. Contractor, I. J. Samudio, Z. Estrov, D. Harris, J. A. McCubrey, S. H. Safe, M. Andreeff and M. Konopleva, A novel ring-substituted diindolylmethane, 1,1-bis[3'-(5-methoxyindolyl)]-1-(*p*-*t*-butylphenyl) methane, inhibits extracellular signal-regulated kinase activation and induces apoptosis in acute myelogenous leukemia, *Cancer Res.*, 2005, **65**, 2890–2898.
- 30 M. York, M. Abdelrahim, S. Chintharlapalli, S. D. Lucero and S. Safe, 1,1-Bis(3'-Indolyl)-1-(*p*-Substitutedphenyl)methanes Induce Apoptosis and Inhibit Renal Cell Carcinoma Growth, *Clin. Cancer Res.*, 2007, **13**, 6743–6752.
- 31 For selected examples using chemical oxidants, see: (a) J.-C. Wu, R.-J. Song, Z.-Q. Wang, X.-C. Huang, Y.-X. Xie and J.-H. Li, Copper-Catalyzed C–H Oxidation/Cross-Coupling of α -Amino Carbonyl Compounds, *Angew. Chem., Int. Ed.*, 2012, **51**, 3453–3457; (b) W.-T. Wei, R.-J. Song and J.-H. Li, Copper-Catalyzed Oxidative α -Alkylation of α -Amino Carbonyl Compounds with Ethers via Dual C(sp³)-H Oxidative Cross-Coupling, *Adv. Synth. Catal.*, 2014, **356**, 1703–1707; (c) C. Huo, H. Xie, M. Wu, X. Jia, X. Wang, F. Chen and J. Tang, CBr₄-mediated cross-dehydrogenative coupling reaction of amines, *Chem. – Eur. J.*, 2015, **21**, 5723–5726; (d) H. E. Ho, Y. Ishikawa, N. Asao, Y. Yamamoto and T. Jin, Highly efficient heterogeneous aerobic cross-dehydrogenative coupling via C–H functionalization of tertiary amines using a nanoporous gold skeleton catalyst, *Chem. Commun.*, 2015, **51**, 12764–12767; (e) B. Dutta, V. Sharma, N. Sassu, Y. Dang, C. Weerakkody, J. Macharia, R. Miao, A. R. Howell and S. L. Suib, Cross dehydrogenative coupling of *N*-aryltetrahydroisoquinolines (sp³ C–H) with indoles (sp² C–H) using a heterogeneous mesoporous manganese oxide catalyst, *Green Chem.*, 2017, **19**, 5350–5355; (f) Y. Liu, C. Wang, D. Xue, M. Xiao, C. Li and J. Xiao, Reactions Catalysed by a Binuclear Copper Complex: Aerobic Cross Dehydrogenative Coupling of *N*-Aryl Tetrahydroisoquinolines, *Chem. – Eur. J.*, 2017, **23**, 3051–3061; (g) W. W. Liang, T. Zhang, Y. F. Liu, Y. X. Huang, Z. P. Liu, Y. Z. Liu, B. Yang, X. C. Zhou and J. M. Zhang, Polydimethylsiloxane sponge-supported nanometer gold: highly efficient recyclable catalyst for cross-dehydrogenative coupling in water, *ChemSusChem*, 2018, **11**, 3586–3590.
- 32 For selected examples using visible-light photoredox catalysis, see: (a) D. B. Freeman, L. Furst, A. G. Condie and C. R. J. Stephenson, Functionally diverse nucleophilic trapping of iminium intermediates generated utilizing visible light, *Org. Lett.*, 2012, **14**, 94–97; (b) Z.-Q. Wang, M. Hu, X.-C. Huang, L.-B. Gong, Y.-X. Xie and J.-H. Li, Direct α -Arylation of α -Amino Carbonyl Compounds with Indoles Using Visible Light Photoredox Catalysis, *J. Org. Chem.*, 2012, **77**, 8705–8711; (c) Q. Y. Meng, J. J. Zhong, Q. Liu, X. W. Gao, H. H. Zhang, T. Lei, Z. J. Li, K. Feng, B. Chen, C. H. Tung and L. Z. Wu, A cascade cross-coupling hydrogen evolution reaction by visible light catalysis, *J. Am. Chem. Soc.*, 2013, **135**, 19052–19055; (d) C. J. Wu, J. J. Zhong, Q. Y. Meng, T. Lei, X. W. Gao, C. H. Tung and L. Z. Wu, Cobalt-catalyzed cross-dehydrogenative coupling reaction in water by visible light, *Org. Lett.*, 2015, **17**, 884–887; (e) X.-W. Gao, Q.-Y. Meng, J.-X. Li, J.-J. Zhong, T. Lei, X.-B. Li, C.-H. Tung and L.-Z. Wu, Visible Light Catalysis Assisted Site-Specific Functionalization of Amino Acid Derivatives by C–H Bond Activation without Oxidant: Cross-Coupling Hydrogen Evolution Reaction, *ACS Catal.*, 2015, **5**, 2391–2396; (f) X. Guo, B. R. Shao, W. F. Jiang and L. Shi, The photocatalyst-free cross-dehydrogenative coupling reaction enabled by visible-light direct excitation of substrate, *J. Org. Chem.*, 2021, **86**, 15743–15752.
- 33 For selected examples using electrochemical oxidation, see: (a) P. Wang, S. Tang, P. Huang and A. Lei, Electrocatalytic oxidant-free dehydrogenative C–H/S–H cross-coupling,



- Angew. Chem., Int. Ed.*, 2017, **56**, 3009–3013; (b) J. H. Wang, X. B. Li, J. Li, T. Lei, H. L. Wu, X. L. Nan, C. H. Tung and L. Z. Wu, Photo-electrochemical cell for P–H/C–H cross-coupling with hydrogen evolution, *Chem. Commun.*, 2019, **55**, 10376–10379; (c) W. X. Xie, N. Liu, B. Gong, S. L. Ning, X. Che, L. L. Cui and J. B. Xiang, Electrochemical cross-dehydrogenative coupling of *N*-aryl-tetrahydroisoquinolines with phosphites and indole, *Eur. J. Org. Chem.*, 2019, **2019**, 2498–2501.
- 34 A. Saeed, D. Shahzad, M. Faisal, F. A. Larik, H. R. El-Seedi and P. A. Channar, Developments in the synthesis of the antiplatelet and antithrombotic drug (*S*)-clopidogrel, *Chirality*, 2017, **29**, 684–707.
- 35 S. Aalla, G. Gilla, D. S. Metil, R. R. Anumula, P. R. Vummenthala and P. R. Padi, Process improvements of prasugrel hydrochloride: an adenosine diphosphate receptor antagonist, *Org. Process Res. Dev.*, 2012, **16**, 240–243.
- 36 A. A. Festa, L. G. Voskressensky and E. V. Van der Eycken, Visible light-mediated chemistry of indoles and related heterocycles, *Chem. Soc. Rev.*, 2019, **48**, 4401–4423.
- 37 For selected examples: (a) M. N. Hopkinson, A. Gómez-Suárez, M. Teders, B. Sahoo and F. Glorius, Accelerated Discovery in Photocatalysis Using a Mechanism-Based Screening Method, *Angew. Chem., Int. Ed.*, 2016, **55**, 4361–4366; (b) A. Gieseler, E. Steckhan, O. Wiest and F. Knoch, Photochemically Induced Radical-Cation Diels-Alder Reaction of Indole and Electron-Rich Dienes, *J. Org. Chem.*, 1991, **56**, 1405–1411; (c) S. Lerch, L.-N. Unkel and M. Brasholz, Tandem Organocatalysis and Photocatalysis: An Anthraquinone-Catalyzed Indole-C3-Alkylation/Photooxidation/1,2-Shift Sequence, *Angew. Chem., Int. Ed.*, 2014, **53**, 6558–6562; (d) C. Zhang, S. Li, F. Bureš, R. Lee, X. Ye and Z. Jiang, Visible light photocatalytic aerobic oxygenation of indoles and pH as a chemoselective switch, *ACS Catal.*, 2016, **6**, 6853–6860; (e) W. Schilling, Y. Zhang, D. Riemer and S. Das, Visible-light-mediated dearomatisation of indoles and pyrroles to pharmaceuticals and pesticides, *Chem. – Eur. J.*, 2020, **26**, 390–395.
- 38 H. G. Roth, N. A. Romero and D. Nicewicz, Experimental and Calculated Electrochemical Potentials of Common Organic Molecules for Applications to Single-Electron Redox Chemistry, *Synlett*, 2016, **27**, 714–723.
- 39 P. Kohls, D. Jadhav, G. Pandey and O. Reiser, Visible light photoredox catalysis: generation and addition of *N*-aryltetrahydroisoquinoline-derived α -amino radicals to Michael acceptors, *Org. Lett.*, 2012, **14**, 672–675.
- 40 For selected examples (a) W. Liang, T. Zhang, Y. Liu, Y. Huang, Z. Liu, Y. Liu, B. Yang, X. Zhou and J. Zhang, Polydimethylsiloxane Sponge-Supported Nanometer Gold: Highly Efficient Recyclable Catalyst for Cross-Dehydrogenative Coupling in Water, *ChemSusChem*, 2018, **11**, 3586–3590; (b) G. Kumar, P. Solanki, M. Nazish, S. Neogi, R. I. Kureshy and N. H. Khan, Covalently Hooked EOSIN-Y in a Zr(IV) Framework as Visible-Light Mediated, Heterogeneous Photocatalyst for Efficient C–H Functionalization of Tertiary Amines, *J. Catal.*, 2019, **371**, 298–304; (c) G. Kumar, S. R. Dash and S. Neogi, Dual-Catalyst Engineered Porous Organic Framework for Visible-Light Triggered, Metal-free and Aerobic sp^3 C–H Activation in Highly Synergistic and Recyclable Fashion, *J. Catal.*, 2021, **394**, 40–49.
- 41 (a) P. S. Baran and J. M. Richter, Direct Coupling of Indoles with Carbonyl Compounds: Short, Enantioselective, Gram-Scale Synthetic Entry into the Hapalindole and Fischerindole Alkaloid Families, *J. Am. Chem. Soc.*, 2004, **126**, 7450–7451; (b) P. S. Baran and J. M. Richter, Enantioselective Total Syntheses of Welwitindolinone A and Fischerindoles I and G, *J. Am. Chem. Soc.*, 2005, **127**, 15394–15396; (c) P. S. Baran and J. M. Richter, Enantiospecific Total Synthesis of the Hapalindoles, Fischerindoles, and Welwitindolinones *via* a Redox Economic Approach, *J. Am. Chem. Soc.*, 2008, **130**, 17938–17954; (d) P. S. Baran, T. J. Maimone and J. M. Richter, Total Synthesis of Marine Natural Products without Using Protecting Groups, *Nature*, 2007, **446**, 404–408.
- 42 S. Imm, S. Bähn, A. Tillack, K. Mevius, L. Neubert and M. Beller, Selective Ruthenium-Catalyzed Alkylation of Indoles by Using Amines, *Chem. – Eur. J.*, 2010, **16**, 2705–2709.

